

IN-43-CR

174940

P-14

Final Report, June 1993

for

**Investigation of a Geodesy Coexperiment to
the Gravity Probe B Relativity Gyroscope
Program**

(NAG 5 -1155)

Submitted to the Earth Sciences Division of the
National Aeronautics and Space Administration
June 25, 1993

by

The W. W. Hansen Laboratories of Physics
Stanford University

C . W. F. Everitt
& Professor in the High Energy
Physics Laboratories (Research)
Principal Investigator,
Gravity Probe B

Bradford W. Parkinson
Professor of Aeronautics
Astronautics (Research)
and H. E. P. L.
Program Manager,
Gravity Probe B

W. W. Hansen Lab. of Physics
Stanford University
Stanford, CA. 94305

report by

Mark Tapley, PhD candidate in Aeronautics and Astronautics,
Stanford University, Stanford, CA. 94305

N93-29179

Unclas

0174940

63/43

(NASA-CR-193263) INVESTIGATION OF
A GEODESY COEXPERIMENT TO THE
GRAVITY PROBE B RELATIVITY
GYROSCOPE PROGRAM Final Report,
Jun. 1993 (Stanford Univ.) 14 p

Table of Contents

- I. Introduction
- II. Results
- III. Contributions
- IV. Conclusion

I. Abstract

Geodesy is the science of measuring the gravitational field of and positions on the Earth. Estimation of the gravitational field via gravitation gradiometry, the measurement of variations in the direction and magnitude of gravitation with respect to position, is this dissertation's focus.

Gravity Probe B (GP-B) is a Stanford satellite experiment in gravitational physics. GP-B will measure the precession the rotating Earth causes on the space-time around it by observing the precessions of four gyroscopes in a circular, polar, drag-free orbit at 650 km altitude. The gyroscopes are nearly perfect niobium-coated spheres of quartz, operating at 1.8 K to permit observations with extremely low thermal noise. The permissible gyroscope drift rate is miniscule, so the torques on the gyros must be tiny. A drag-free control system, by canceling accelerations caused by nongravitational forces, minimizes the support forces and hence torques.

The GP-B system offers two main possibilities for geodesy. One is as a drag-free satellite to be used in trajectory-based estimates of the Earth's gravity field. We described calculations involving that approach in our previous reports, including comparison of laser only, GPS only, and combined tracking and a preliminary estimate of the possibility of estimating relativistic effects on the orbit.

The second possibility is gradiometry. This technique has received a more cursory examination in previous reports, so we concentrate on it here. We explore the feasibility of using the residual suspension forces centering the GP-B gyros as gradiometer signals for geodesy. The objective of this work is a statistical prediction of the formal uncertainty in an estimate of the Earth's gravitation field using data from GP-B. We perform an instrument analysis and apply two mathematical techniques to predict uncertainty. One is an analytical approach using a flat-Earth approximation to predict geopotential information quality as a function of spatial wavelength. The second estimates the covariance matrix arising in a least-squares estimate of a spherical harmonic representation of the geopotential using GP-B gradiometer data.

The results show that the GP-B data set can be used to create a consistent estimate of the geopotential up to spherical harmonic degree and order 60. The formal uncertainty of all coefficients between degrees 5 and 50 is reduced by factors of up to 30 over current satellite-only estimates and up to 7 over estimates which include surface data. The primary conclusion resulting from this study is that the gravitation gradiometer geodesy coexperiment to GP-B is both feasible and attractive.

II. Results

This section presents the results of calculations estimating the statistical uncertainty in a geopotential field model obtained by reducing data from the GP-B gradiometry coexperiment. We rely on an extensive instrument analysis described in Chapter IV of Mr. Tapley's forthcoming dissertation for the precision of the GP-B gradiometer; we assume it to be 0.05 Eötvös as we concluded there. We also assume an 18-month period of data collection with one reading collected each second during that period.¹ The results we give address the question of statistical uncertainty in determination of coefficients rather than absolute accuracy. We will devote more attention to the subject of verification at the conclusion of this section. The approximations we used all agree closely in their prediction of the uncertainty in the gravitation field. They indicate that the GP-B field will contain statistical uncertainties as much as 30 times smaller than the best current fields which use only satellite tracking data and up to 7 times better than the best current global fields which include surface gravimetry.

The flat-Earth approximation [Breakwell, 1979] is a simple analytical method to predict the reduction factor F in statistical uncertainty in geopotential coefficient estimates resulting from inclusion of a single new set of observations in the estimation process. F is given by the equation

$$F = \sqrt{\frac{1}{2\pi} \int_0^{2\pi} \frac{d\alpha}{1 + \phi_{U_0}(\omega) H^T(-\bar{\omega}) \Phi_W^{-1} H(\bar{\omega})}} \quad (6.1)$$

where $\phi_{U_0}(\omega)$ represents the *a priori* information on the geopotential, Φ_W represents the noise in the new observations, and H is a vector describing the relationship between the gravitation field and the instrument output. The *a priori* information in all of our plots which use the flat-Earth approximation comes from Kaula's rule [Kaula, 1966]. We multiply Kaula's original formula by 0.7 to facilitate comparison with the results of Lerch et al [Lerch 1992]. A fuller description of the flat-Earth technique and derivation of the H function for gradiometers appears in my forthcoming dissertation.

GP-B senses only the axial strain component of the gradient tensor. This component corresponds to the local vertical strain (Γ_{zz}) in topocentric coordinates twice per orbit. At two other points in the orbit, it corresponds to the local horizontal along-track strain (Γ_{yy}). In between, it is a combination of those and the vertical/along-track shear component of the tensor. The flat-Earth approximation is not capable of simulating this variation in sensing, so there is a question of what function to use for H . We select the Γ_{zz} function for most of the plots we present because the equatorial latitudinal zones, where GP-B is in a Γ_{zz} configuration, comprise the greatest fraction of the Earth's surface area (though they are also primarily covered by water). Figure VI.1 shows plots for the Γ_{zz} configuration and for the Γ_{yy} configuration.

The horizontal axis on Figure VI.1 is presented in terms of degree of the

¹The instrument and data pathway are capable of meeting this rate of observations. A lower rate would increase the statistical uncertainty of the estimates while reducing demands on the satellite systems.

spherical harmonic representation of the geopotential. The flat-Earth approximation is actually an analytical function of spatial wavelength. We convert wavelength to degree n by the equation

$$\omega = n / R_{\text{earth}} \quad (6.2)$$

so that the plot is more easily compared to other approximations. We display degrees starting with 10 rather than 2 because we do not expect the flat-Earth approximation to be accurate for degrees lower than 10. The vertical axis presents the average uncertainty in coefficients of the given degree. The results of the flat-Earth approximation are derived by numerical quadrature of Equation (6.1) using Equation (6.2) to produce ω for a given degree. The result (F) of Equation (6.1) is multiplied by the *a priori* (Kaula's Rule times 0.7) to give the plotted value of the statistical uncertainty in coefficients of degree n for a gravitation field estimate using GP-B data. This procedure precludes negative predictions for the uncertainty.

We include Kaula's rule on the plot so that the value of F may be read off by dividing the two quantities. The *a priori* becomes the dominant factor in the uncertainty at approximately degree 60. Another interpretation of this is that the uncertainty in coefficients has become as large as the coefficients themselves, since we are using Kaula's rule to represent the size of the coefficients. This feature of the plot forms the basis for our claim that the field GP-B can produce will be significant up to degree and order 60.

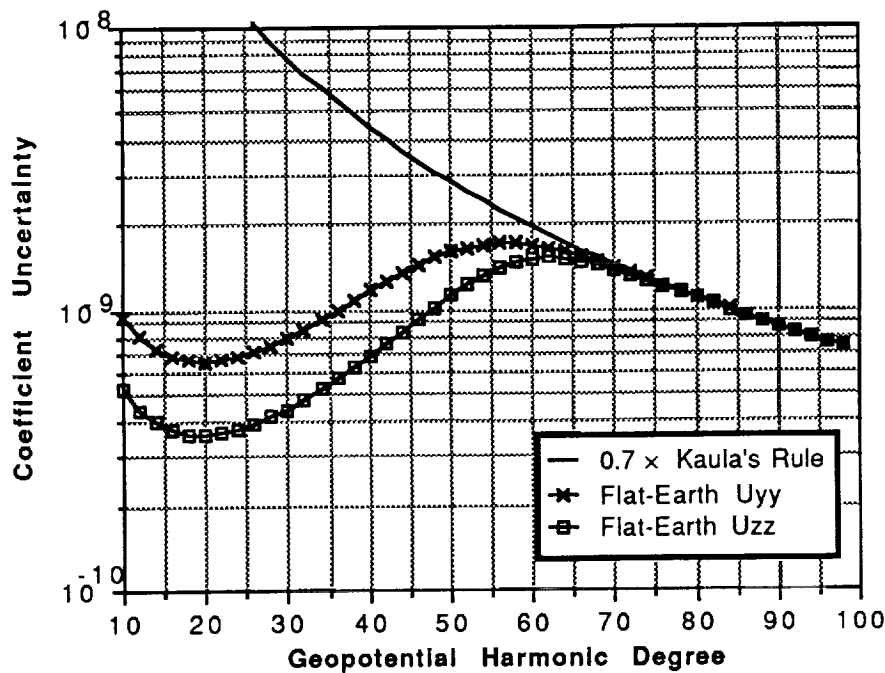


Figure VI.1 Flat-Earth Predictions of Coefficient Uncertainty for GP-B Geopotential Estimate

A more realistic evaluation of statistical uncertainty in the estimate of the geopotential field from GP-B is provided by a covariance analysis we performed using Mathematica. This approach reconstructs the covariance matrix associated with a

least-squares estimate of the geopotential coefficients using gradient data. If the matrix H represents the relationship between the geopotential coefficients and the gradient readings and R represents the accuracy of the gradiometer, the covariance matrix is expressed as

$$P = (H^T R^{-1} H)^{-1} \quad (6.3)$$

The covariance technique's advantages over the flat-Earth approximation are that it assumes readings with a realistic geographical distribution and orientation, and that it produces an estimate of the uncertainty associated with each coefficient in the expansion rather than an estimate averaged over all coefficients at a given degree. The derivation and implementation of this technique are discussed in the dissertation.

Figure VI.2 shows the results of the covariance technique grouped by degree and order. In this plot, the cosine and sine components for each degree and order are squared, summed, and the square root taken to produce the plotted value. The horizontal axis is the order, the axis extending out of the page degree, and the vertical axis the logarithm of the predicted uncertainty at that degree and order.

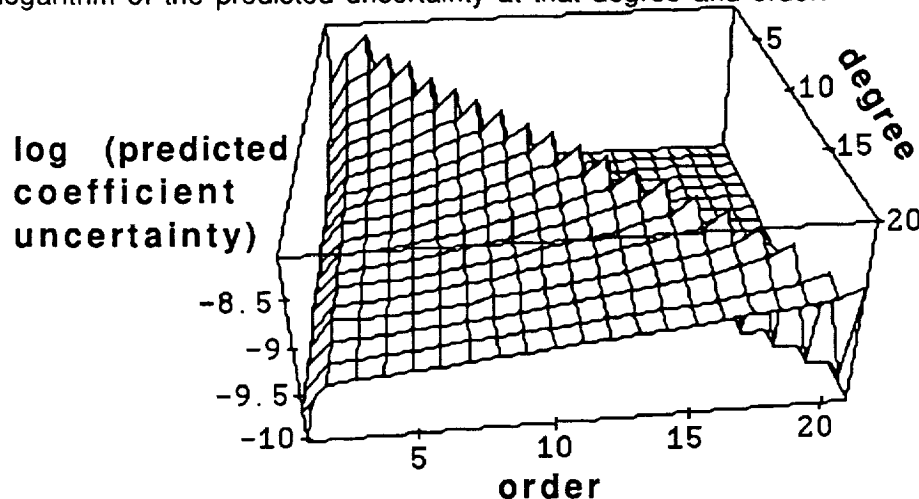


Figure VI.2 Covariance Predictions of Uncertainty by Degree and Order

One drawback of the covariance approach is that it requires a large amount of computation to make covariance matrix estimates for higher degrees. Using the available computing resources, it was not practical to estimate the full covariance matrix for solutions of degree 21 or above. It is feasible, however, to make estimates of the covariances associated with coefficients for only a few degrees of a higher-degree estimate. For example, we made a run estimating the covariances associated with coefficients of all orders at degrees 49 and 50 only. A feature of this technique is that the predicted covariances for the partial solutions are lower than the predicted covariance for the same degree in a full solution. We compensated for this by multiplying the effective number of observations by the factor n_p / n_f , where n_p is the number of coefficients solved for in the partial estimate and n_f the number of coefficients in a full estimate of the same degree. We plot below results for both the compensated and the uncompensated estimates.

The estimate of the covariances for the full degree and order field shows an attribute typical of covariance solutions for large systems of spherical harmonics [Schrama, 1992], [Pavlis, 1989]. The average covariances for the highest few degrees (19 and 20, in our case) are lower than the trend indicated by the preceding degrees. Such decreases have been found in many large gravitation field solutions and do not affect the validity of the estimates.

The plots below show the results of the covariance analysis in the same format as the flat-Earth presentation. The horizontal axis is presented in degrees as before, and in this case no conversion from spatial frequency is needed. The vertical axis represents an arithmetical average of the covariances associated with coefficients of every order at the given degree. The plot points were obtained by simply adding up the covariances (all of which are positive by the nature of the covariance matrix) and dividing by the number of addends at that degree. Figure VI.3 shows the flat-Earth estimate compared to the partial and full covariance estimates.

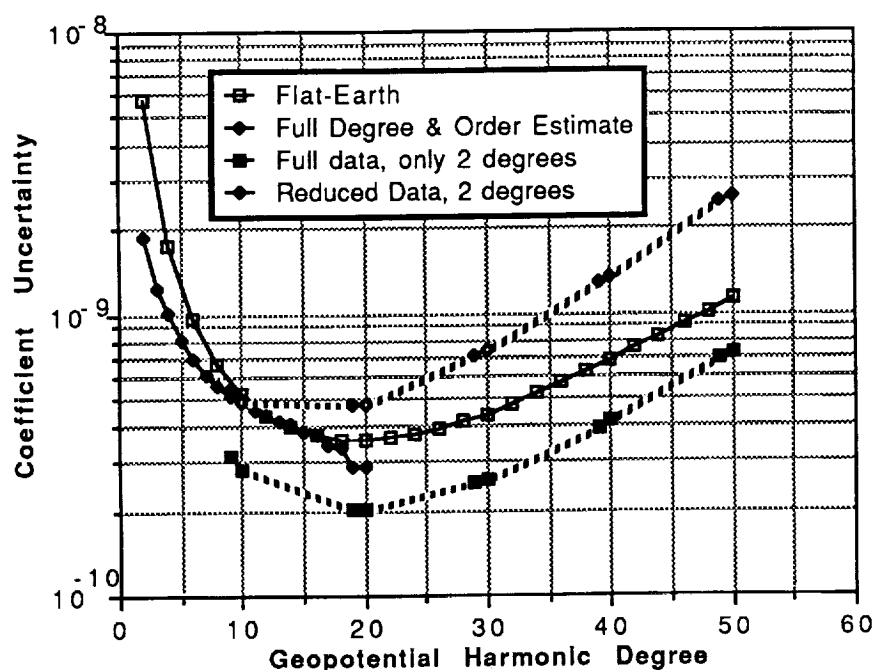


Figure VI.3 Results of Covariance Estimate of GP-B Performance

The last approximation we use to predict GP-B's performance in estimating geopotential coefficients is attributed to Schaechter [Schaechter, 1977], which we describe in Section V.E. It is similar to the flat-Earth approximation in that it does not take into account geographical location of the gradiometer, but assumes uniform distribution of readings over the entire globe. It also assumes a Γ_{zz} gradiometer. Its result, like the flat-Earth approximation, is a plot of predicted geopotential coefficient uncertainty as a function of degree. The points we plot are derived by evaluating Equation (5.34) at each degree. The difference between the flat-Earth and Schaechter's approximations is explained by two causes. The first is the factor $1/((n+1)(n+2))$ in Equation (5.34) which the flat-Earth approximation rounds to $1/n^2$. The second is the use of the *a priori* information in the flat-Earth, which causes the drop-off in

uncertainties above degree 50.

For a comparison between the results we predict and the current state of the art, we will use the GEM-T3 and GEM-T3S geopotential models produced by Goddard Space Flight Center. [Lerch 1992]. These are both spherical harmonic representations of the Earth's gravitational potential field complete to degree and order 50. GEM-T3S uses only satellite tracking data in its calculations, while GEM-T3 adds data from surface gravimetry and satellite altimetry. The GEM-T3 model has lower expected errors in its coefficients due to the increased amount and quality of the data that went into it. In addition, it yields orbit determination improvements over GEM-T3S. However, the geographical concentration of its surface data produces geographical correlations in its statistical uncertainties [Kogan 1993]. For direct comparison of satellite data to satellite data, GEM-T3S is more appropriate, while for comparison to the best information available GEM-T3 is better. The uncertainties in the GEM-T3 and GEM-T3S models are plotted as RMS coefficient error by degree. These plots include the influence of data set down-weighting to account for systematic and modelling errors.

Figure VI.4 displays the Flat-Earth and Covariance predictions of coefficient uncertainty and Schaechter's approximation on the same plot with the GEM-T3 and GEM-T3S. The horizontal axis is appropriate for all of the plots, with the provision that the flat-Earth must be transformed from spatial wavelength to degree. The vertical axis always represents the uncertainty for coefficients of a given degree. For the flat-Earth and Schaechter approximations, it represents a single uncertainty assigned by degree to the coefficients. For the others, it represents the uncertainty averaged (either RMS or arithmetical average) over all orders at that degree. For the Kaula's rule plot, it represents not uncertainty but expected magnitude of the coefficients. One may find percentage error in coefficients at any degree by dividing the value given by Kaula's rule by the value given by the plot for the pertinent method of prediction (or estimation, in the case of GEM-T3 and GEM-T3S).

One very significant features of Figure VI.4 is that the gradiometer estimate of the gravity field is strongest where the trajectory perturbation estimates are weakest. The gradiometry uncertainties reach a minimum at degree 20 while the GEM-T3S and GEM-T3 uncertainties reach maxima at degrees 20 and 25 respectively. The reason for the difference in the shapes of the plots is the nature of the different measurement systems. Trajectory perturbation analysis is fundamentally an integrating process more sensitive to low-frequency disturbances. Gradiometry is essentially a differentiating process more sensitive to higher frequencies. The minimum in the estimated uncertainties for the gradiometer is due to the attenuation of the effects of the higher harmonics at altitude; a surface gradiometer would have steadily improving performance at increasing degree. The flat-Earth prediction of the GP-B uncertainty, which uses Kaula's rule as an *a priori*, has another local maximum at degree 62. This maximum is due not to the gradiometer information but to the increasing effect of the *a priori*, just as the decreasing uncertainty in the GEM-T3S coefficients above degree 20 is due to the use of Kaula's rule to limit the predicted uncertainties in the solution (though GEM-T3 also benefits at high degree from the inclusion of surface data). Schaechter's approximation does not contain any *a priori* or limiting value, so it does not show a maximum at that point.

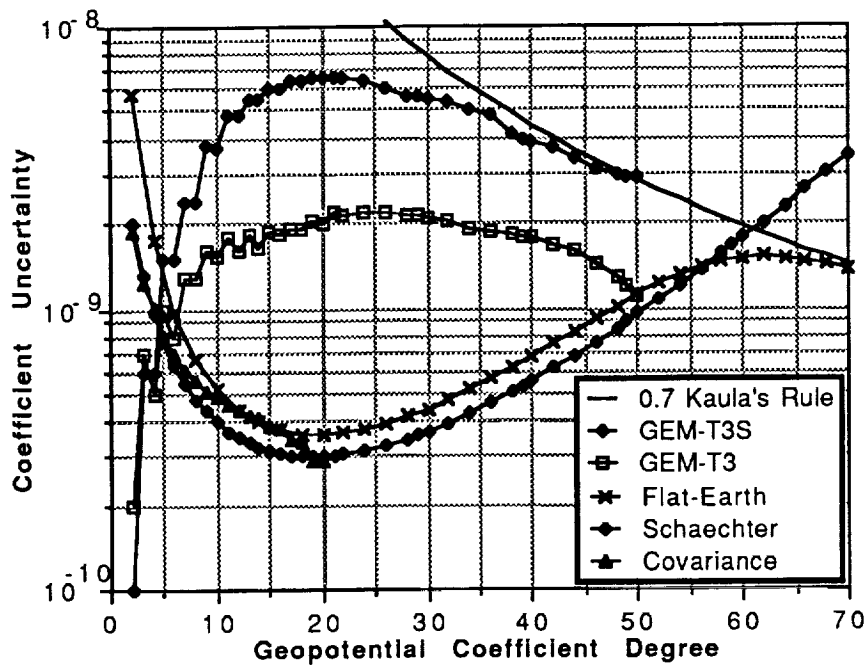


Figure VI.4 Comparison of Predictions of GP-B Performance.

We should examine the fundamental causes for the significant formal improvement these results show over the current state of the art. The sensing system is the first cause. The superconducting GP-B instruments, though not designed for gradiometry, are sufficiently sensitive with a low thermal noise level to make gradient measurements equaling almost any Earth-bound instrument. The second cause is the distribution and rate of the data. A data rate of one measurement every second, round the clock, is possible. This rate over 18 months for GP-B produces an excellent data set for estimating the Earth's gravitational field. The data are well distributed because the orbit of GP-B is polar. The entire Earth is covered with gradient observations, though the vertical (Γ_{zz}) gradient observations are concentrated near the equator while the Γ_{yy} observations are near the poles. The altitude is fairly low; its semi-major axis is smaller than those of most of the satellites used in the computation of GEM-T3S; therefore it is sensitive to higher-degree potential variations. Its period may easily be adjusted so that it attains sufficiently low spacing between ground tracks but also allows repeated readings at the same locations for calibration purposes. Furthermore, the drag-free control system minimizes common-mode disturbances on the instrument. Finally it is a gradiometer, which is a differential instrument as opposed to the integrating instruments used for satellite geodesy to date. This makes it relatively more sensitive to higher degree coefficients. With this combination of attributes, the single GP-B satellite is able to make a substantially better estimate of the gravitational field than any previous system or combination of systems.

One further feature of the GP-B system which is very beneficial to the gradiometry coexperiment is the GPS receiver. The GPS system allows us to orient and locate readings in a topocentric frame common to many other geodetic observations

assuming a sufficient number of antennas are on the GP-B spacecraft. It also allows continuous monitoring of the position of GP-B during the entire course of the mission with accuracy more than sufficient for the gradiometry coexperiment.

In this section we have discussed the statistical uncertainty which will be associated with the gravity field estimated from GP-B gradiometer data. Except for the GEM-T3 and GEM-T3S results, all of the approaches presented here give variances which scale as

$$\sigma_0 = \sigma_i (t / D)^{1/2} \quad (6.4)$$

where σ_i is the variance associated with a single reading, t is the time between readings, and D is the duration of the mission. Obviously, at some point modelling errors and systematic errors will become more significant than the statistical uncertainty. We have not addressed this issue. Experience gained with the GEM-T3S model indicates that for trajectory perturbation analysis, systematic and unmodeled error are larger than the statistical uncertainty in the solution, with most of the error coming from surface forces acting on the satellite to change its trajectory. That error source will not affect the GP-B solution, but others undoubtedly could. We therefore cannot address the question of accuracy (as opposed to precision) of the geopotential estimate GP-B will produce without some standard against which to compare it.

Two possibilities for standards by which to evaluate the gradiometer results are estimates produced by trajectory analysis, such as GEM-T3S, and estimates produced by surface observations. The surface observations themselves may be gravimetry surveys conducted on the ground or from aircraft or ocean-surface topography maps created by satellite radar altimetry. The first should have statistical uncertainties lower than the GP-B field at low degrees, and the last at high degrees. GP-B itself is expected to provide a very high quality gravitation field estimate for low degrees though analysis of perturbations to its trajectory [Tapley, 1989; Breakwell, 1989]. The TOPEX/Poseidon mission underway at this writing is expected to provide high-quality ocean topography maps. None of these are absolute standards of comparison. At best they can only offer agreement over the degrees where they apply. Nevertheless, comparison to independent standards such as ground gravimetry and radar ocean topography surveys is a necessary consistency check for the GP-B estimation process.

III. Contributions of this Investigation

Improvement of the formal uncertainty in coefficients representing the Earth's gravitational field when extended downward to a topocentric frame is the goal for the geodesy coexperiment. I have shown that it is desirable and achievable using only minor modifications to the procedures and equipment already necessary for GP-B, while adding only a relatively small increase to the data downlink requirements. To do so, I have made several significant contributions to the state of the art.

The most original part of this work has been a complete analysis of the GP-B gyroscope suspension systems as applied to the problem of gravitation gradient measurement. The entire GP-B experiment was designed to observe the angle between the optical axis of the telescope and the spin axes of the gyros, with no consideration for gravitation gradiometry. That it can function so well as a gradiometer is a consequence of the highly demanding nature of the primary experiment which requires a cryogenic superconducting instrument, and also of the fact that it must carry a GPS receiver to insure a polar orbit. Nevertheless, its design means that a careful analysis and innovative approaches to problems of observability and calibration were required to establish the viability of the coexperiment. The instrument analysis I performed was necessary in developing the concept of the coexperiment.

The first part of the instrument analysis was to identify and quantify the error sources affecting the gradient measurement; the results of this process appear in Table 1. This work identifies the features of the instrument design which have the greatest impact on the gradiometry coexperiment. Subsequent to that effort, I also suggested ways to improve the geodesy coexperiment, and discussed their effect on the relativity experiment. The analysis of GP-B instrument design from a gradiometry perspective is unique and may assist in determining GP-B's final configuration. An example of this is the advantage of a digital suspension compensation system over an analog one, to remove the need for an A/D converter in the gradient data pathway.

In the instrument analysis, I also specified exactly what measurements are necessary for the success of and what backup or redundant messages are desirable for the gradient coexperiment, and what the resulting downlink data rate will be. This information is vital in designing the support systems on GP-B, including data storage and communications bandwidth. It is impossible at this stage to specify what fraction of the gradient data is subsumed by the housekeeping data stream, but it should be easy to resolve that when the housekeeping data requirements are established.

Error in Axial Gradient Measurements	0.05 E
Instrument Errors	0.05 E
scale factor (quantization) (0.000017)	0.017 E
nonlinearity (Specified; calibration complexity)	< 0.02 E
bias (calibration)	0.0027 E
quantization (single obs. error; less with oversampling)	0.05 E
cross-coupling (calibration)(centrifugal coupling into axial)	0.0005 E
Specific Force Gradient Noise	
radial dynamics	0.44 E
relative motion of gyros	~ 0
tangential rotation (roll control)	0.44 E
Coriolis acceleration (" , spec. for gyro relative motion)	0.00018 E
centripetal acceleration (roll control)	0.00008 E
common acceleration (scale factor calibrated)	0.000 017 E
axial dynamics	0.0023 E
relative motion of gyros	~ 0
tangential rotation	0.0023 E
Coriolis acceleration (spec. for gyro relative motion)	0.000 000 94 E
centripetal acceleration	0.000 053E
common acceleration (scale factor calibrated)	0.000 017 E
spacecraft solid dynamic gradients	< 0.0057 E
spacecraft fluid dynamic gradients	specified
s/c static gradients	0.0008 E
reference system/positioning error	< 0.000 35 E
reference system	~ 0
orientation (axial alignment)	< 0.000 35 E
systematic positioning error	$\Delta C_n = 6.6 \times 10^{-11}$
calculations	(see Ch. VI)

Table IV.5 Error Budget for GP-B Gravitation Gradiometry

A crucial contribution I made was the calibration scheme which will allow the suspensions to act reliably as absolute specific force meters. I showed that the point-mass (GM) and oblateness (C_{20}) terms in the Earth's gravitation spectrum provide a suitable input to the suspensions to calibrate them to the accuracy needed for the gradiometer coexperiment. Uncertainties and disagreements in estimates of both quantities are already small enough that they are inconsequential in the calibration process. The specific forces they exert on the gyros occur at a range of frequencies from zero up to 0.02 rad/s if GP-B rolls at a rate of one revolution every 10 minutes. The upper limit is also the threshold of the frequency range of inputs valuable for the gradiometry coexperiment, so in this case the calibrating input is a good match for the desired signal in terms of bandwidth. I obtained an estimate showing that the residual

uncertainty in bias and alignment parameters in the suspension using this calibration scheme is easily small enough for the gradient coexperiment. Without such a calibration scheme, the results obtained by the gradient coexperiment could not be reliable. With it, calibrated instrument errors become a minor consideration in the final error analysis.

I also examined the attitude control system of GP-B to determine whether errors in the attitude would contaminate the gradient sensing or interfere with the calibration. The conclusion is that they will not for the current system. Given that the relativity mission requires an external reference (its guide star), it is difficult to imagine a control system such that attitude errors are more significant than errors in estimates of dynamical motion. Refinement of roll rate control or observation is the single most valuable improvement to the system in terms of the geodesy coexperiment.

Once the instrumentation feasibility was established, we addressed the question of what improvement in geodesy could be expected with GP-B. In this area the mathematical treatments presented above were major contributions.

The covariance analysis also furthered the gradiometry coexperiment by supporting the assertion that the GP-B gradiometer provides enough information to give a consistent estimate of a geopotential field complete to a given degree and order. The GP-B instrument, like others proposed for ARISTOTELES and STEP, is a partial-tensor instrument. The concept of statistically estimating a gravitation field model from partial tensor observations must provoke skepticism in a careful observer, and the question of whether the field is recoverable with a partial-tensor instrument is therefore critical to many gravitation gradiometer missions.

The covariance analysis allowed me to run many cases with varying combinations of orbit, measured gradient component, and number and distribution of observations. It represents the case of GP-B very well, with its varying combination of observed (topocentric) gradient components and polar concentration of data. The result of the covariance analysis is reasonable. As in Schaechter's work, the gravitation field model can be estimated if a sufficient number and distribution of observations are used. A non-invertible information matrix is a clear indicator that an insufficient number of readings is being used and the estimate will not be consistent. The number of readings GP-B is expected to collect is well in excess of the number needed for a gravitation field estimation such as we describe above, complete to degree and order 60. The results of the covariance analysis should allay doubts about the GP-B gradiometer's ability to provide sufficient data to make a consistent estimate of a full set of geopotential coefficients to at least degree 60.

IV. Conclusion

Our conclusion is that the gradiometry coexperiment to GP-B is a valid means of obtaining significant geopotential information about the Earth at relatively low cost. The trajectory-based approach to geodesy has been documented in previous publications [Tapley, 1989], [Breakwell, 1989] and will be very effective with GP-B. The gradiometry approach is novel but should enjoy similar success; detailed analysis of its capabilities appears in the dissertation of Mr. Tapley due out this summer. Results presented above from that document show that the gradiometry and trajectory techniques are complementary. The opportunity to compare the two techniques on a single satellite will be particularly valuable for the planning of future missions in Earth Sciences.

We wish to express our gratitude to the Earth Sciences Division of the National Aeronautics and Space Administration for making this work possible.

References:

Breakwell, John V., 'Satellite Determination of Short Wavelength Gravity Variations', *Journal of Astronautical Sciences*, Vol XXVII, #4, pp. 329-344, (Oct.-Dec. 1979)

Breakwell, John V., Tapley, Mark, Everitt, C.W.Francis 'Impact of the Gravity Probe B mission on Satellite Navigation and Geodesy', *Proceedings of the IAF conference on Astrodynamics*, September, 1989

William B. Kaula. "Theory of Satellite Geodesy", Blaisdell Publishing Company, Waltham, Massachusetts, 1966.

Kogan, Mikhail G., McNutt, Marcia K. "Gravity Field over Northern Eurasia and Variations in the Strength of the Upper Mantle" *Science*, vol. 259, 22 January 1993.

Lambeck, Kurt (1988) "Geophysical Geodesy", Clarendon Press, Oxford

Lerch, F.G.; Nerem, R.S.; Putney, B.H.; Felsentreger, T.L.; Sanchez, B.V.; Klosko, S.M.; Patel, G.B.; Williamson, R.G.; Chinn, D.S.; Chan, J.C.; Rachlin, K.E.; Chandler, N.L.; McCarthy, J.J.; Marshall, J.A.; Luthcke, S.B.; Pavlis, D.W.; Robbins, J.W.; Kapoor, S.; Pavlis, E.C.; "Geopotential Models of the Earth From Satellite Tracking, Altimeter, and Surface Gravity Observations: GEM-T3 and GEM-T3S". NASA Technical Memorandum 104555, Goddard Space Flight Center, Greenbelt, MD, January, 1992.

Nerem, R.S., Tapley, B.D., and Shum, C.K.; "A General Ocean Circulation Model Determined in a Simultaneous Solution with the Earth's Gravity Field"; *Proceedings, IAG Symposium 104 on Sea Surface Topography, the Geoid, and Vertical Datums*, Sept. 1989.

Pavlis, E, and Colombo, O; extensive personal tutoring, 1989.

D. Schaechter, M. Kurosaki, D.B.DeBra, "Study to Develop Gradiometer Techniques", report no. AFGL-TR-78-0046, Dec. 1977, U.S. Air Force Geophysics Laboratory, Hanscom AFB, Massachusetts, 01731

Schrama, E. J. O.; 1992, personal communication.

Tapley, Mark, Breakwell, John V., Everitt, C.W.Francis, 'Contribution of the Gravity Probe B mission to Geodesy and to Satellite navigation', *Proceedings, IAG symposium 105 on satellite geodesy*, Edinburgh, Scotland, August, 1989